Time-resolved photodissociation of p-bromotoluene ion as a probe of ion internal energy

ARTICLE *in* INTERNATIONAL JOURNAL OF MASS SPECTROMETRY AND ION PROCESSES · DECEMBER 1996

DOI: 10.1016/S0168-1176(96)04463-1

3 AUTHORS, INCLUDING:

Seung Koo Shin
Pohang University of Science and Technology
79 PUBLICATIONS **1,347** CITATIONS
SEE PROFILE

Seung-Jin Han
Pohang University of Science and Technology
14 PUBLICATIONS **242** CITATIONS
SEE PROFILE

ELSEVIER International Journal of Mass Spectrometry and Ion Processes 157/158 (1996) 345–355

International Journal of Mass Spectrometry and Ion Processes

Time-resolved photodissociation of *p*-bromotoluene ion as a probe of ion internal energy

Seung Koo Shin[1,2], Seung-Jin Han, Byungjoo Kim

Department of Chemistry, University of California, Santa Barbara, Santa Barbara, CA 93106-9510, USA

Received 22 May 1996; accepted 25 July 1996

Abstract

The unimolecular dissociation of the *p*-bromotoluene radical cation was studied by using Fourier transform ion cyclotron resonance spectrometry. The parent ions were prepared by charge-transfer reactions of toluene-d_8 ions with *p*-bromotoluene. The toluene-d_8 radical cations were produced by two-photon ionization at 266 nm. The photodissociation was accomplished by 532 nm. The *p*-bromotoluene ion dissociates to $C_7H_7^+$ with a loss of Br via one- and two-photon processes. The structures of the $C_7H_7^+$ products were identified by ion–molecule reactions. The dissociation rates were measured by time-resolved photodissociation (TRPD) spectroscopy. The $C_7H_7^+$ products from one-photon dissociation (1PD) were reactive toward toluene-d_8 and yielded $CD_3C_6D_4CH_2^+$, indicating the benzyl ion structure. No unreactive tropylium ions were detected from 1PD. The rate constant of 1PD obtained at the internal energy of 2.43 eV was combined with the photoelectron–photoion coincidence data reported in the internal energy range 2.75–3.33 eV to estimate the activation parameters for the lowest barrier process that led to the benzyl ion exclusively. The two-photon dissociation (2PD) resulted in both the benzyl and tropylium ions with the branching ratio, [benzyl$^+$]/[tropylium$^+$] = 92/8. It appears that the tropylium ion results from the isomerization of the *p*-tolyl ion produced by 2PD via a direct C–Br cleavage. The TRPD spectroscopy was used as a thermometric probe of the average internal energy of the parent ions produced by electron impact. The rates of 1PD were compared as a function of cooling time and pressure to examine the energy cooling processes. The effect of radiative heating of an ICR cell by hot filament on the dissociation rate was also examined.

Keywords: *p*-Bromotoluene; $C_7H_7^+$; Time-resolved photodissociation; Photoionization charge-transfer; Ion thermometry

1. Introduction

In the study of gas phase ion chemistry, it is of fundamental importance to know the internal energy of the reactant ion. It governs the kinetics of uni- and bimolecular reactions and affects the reaction dynamics [1]. The extent of internal excitation depends on ionization, activation, and relaxation processes [1,2]. For example, monoenergetic ions are formed by photoelectron–photoion coincidence (PEPICO) selection [3], while state-selected ions are prepared by two-color resonant multiphoton ionization [4]. Vibrationally hot ions with a broad internal energy distribution are generated by electron impact (EI), while they are thermalized by collisional quenching and radiative relaxation. Both the preparation and

[1] National Science Foundation—Young Investigator, 1994–1999.
[2] Arnold and Mabel Beckman Foundation—Young Investigator, 1994–1996

PII S0168-1176(96)04463-1

excitation of ions in a well-defined internal energy range are needed to achieve the goal of energy-selective chemistry.

In this work, the unimolecular dissociation of the *p*-bromotoluene ion was studied using Fourier transform ion cyclotron resonance (FTICR) spectrometry. The parent ions were prepared in an ICR cell by a photoionization charge-transfer (PICT) method in the absence of radiative heating by hot filament. The PICT ensures the thermalization of the parent ion at room temperature. The thermal parent ions were then optically excited by a laser. The photon energy is converted to an internal energy via a fast internal conversion process. The dissociation rates were measured and the structures of the product ions were identified.

The dissociation of the *p*-bromotoluene ion has been previously studied among other halotoluenes [5–9]. At energies within a few eV of threshold, the $C_7H_7^+$ ions are produced with a loss of Br.

$$p\text{-}CH_3C_6H_4Br^{+\cdot} \rightarrow C_7H_7^+ + Br \quad (1)$$

The structures of $C_7H_7^+$ formed by EI were characterized by Jackson et al. in an ICR spectrometer [5]. The branching ratio, [benzyl$^+$]/[tropylium$^+$], was reported at three different electron energies: 99/1 at 14 eV, 94/6 at 17 eV, and 93/7 at 25 eV, indicating the benzyl ion as the most abundant species. In contrast to the ICR results, McLafferty and coworkers reported a low benzyl ion abundance (18%) from collisional activation (CA) mass spectrometric studies of $C_7H_7^+$ produced by EI of *p*-bromotoluene at 70 eV [6,7]. Stapleton et al. measured the kinetic energy release from the fragmentation of metastable *p*-bromotoluene ions and suggested that the slow dissociation proceeded with rearrangements [8]. Olesik et al. reexamined the structures of $C_7H_7^+$ by CA experiments and investigated the dissociation rates and energetics of reaction 1 by PEPICO experiments [9]. The CA studies of the *p*-bromotoluene ion produced from EI at 70 eV yielded the branching ratios favoring the formation of the tropylium ion; % tropylium: % benzyl: % tolyl = 76:21:3. The PEPICO experiments in the internal energy range 2.75–3.3 eV provided the parameters for the Rice–Ramsberger–Kassel–Marcus (RRKM) model; the activation energy, E_0 = 1.8 eV, and the entropy of activation, $\Delta S^{\ddagger}$(1000 K) = −4.8 eu. The measured kinetic energy release near E_0 was far from being statistical, indicating the presence of a high reverse barrier in the exit channel of the lowest barrier pathway. However, the structural identities of $C_7H_7^+$ resulted from the lowest activation process have not been determined [10–16]. Since the EI employed in the previous ICR and CA studies are not energy-selective, a mixture of $C_7H_7^+$ structures identified from such studies do not necessarily correlate to the lowest activation product. The energy-selective studies are needed for the elucidation of the mechanism of unimolecular dissociation of the *p*-bromotoluene ion in the gas phase.

To achieve the goal of energy-selective studies, the parent ions were prepared by charge-transfer reactions of the toluene-d_8 ions, produced by two-photon ionization (2PI) of toluene-d_8 at 266 nm, with *p*-bromotoluene. In the PICT experiment, there is no radiative heating of the ICR cell by hot filament. The PICT method gains several advantages over EI. First, there are no complications due to the formation of isomeric ions. Secondly, the temperature of molecules in the ICR cell is the same as the housing temperature. Lastly, the positions of ions in the ICR cell are predetermined by an ionization laser path, which allows a good overlap with a photodissociation laser beam. The photoexcitation was accomplished at 532 nm. The wavelength was chosen so as to excite the parent ions above the lowest activation barrier but below the thermochemical threshold for the tolyl ion production at 2.90 eV [9]. The structure of $C_7H_7^+$ was identified from ion–molecule reactions with toluene-d_8 [17]. The dissociation rates were measured from the time-resolved photodissociation (TRPD) experiments. The

laser power dependence of the TRPD spectra was checked to distinguish between one and two-photon processes. The measured dissociation rate was combined with the previous PEPICO results [9] for the refinement of the RRKM parameters.

The rate–energy curve obtained from the RRKM parameters were used to estimate the average internal energy of vibrationally hot ions produced by EI. The TRPD thermometry developed by Dunbar and coworkers [18–31] is one of the most accurate methods for the measurement of ion internal energy in the ICR cell [2]. Herein, we employed the TRPD thermometry for the studies of internal excitation of the *p*-bromotoluene ion produced by EI, the energy cooling processes, and the effect of radiative heating of the ICR cell on the ion internal energy.

2. Experimental

All experiments were performed with a newly constructed FTICR spectrometer. A schematic of an experimental setup is shown in Fig. 1. The instrument consists of a 5.0 T superconducting magnet (Oxford), a stainless steel vacuum chamber differentially pumped by three cryogenic pumps (APD-6, 690 l s^{-1}), and an FT-data system (IonSpec, Omega/486) for the data handling and control electronics. A laboratory-built 2 inch cubic trapping cell [32–34] is made out of 316 stainless steel and mirror polished inside. The ICR cell is mounted at the end of the external ion guide. In the center of trapping plates, there is a 0.325 inch hole for an optical access. A thermionic filament made out of a 30 μm thick, 0.762 mm wide Re ribbon is mounted vertically across the hole in the trapping plate. The laser beam is obstructed only by a 30 μm thick line. The background pressure is typically below 9.0×10^{-10} Torr after bakeout. Gaseous samples were admitted to the ICR chamber through either a leak valve (Varian, 951-5106) or a laboratory-built pulsed valve using a piezo-translator, both of which led to the ICR cell through separate electropolished stainless steel tubes. The pressure in the ICR chamber was typically measured using a Schultz-Phelps (S-P) ion gauge [35] mounted next to the transmitter plates. The S-P gauge reading was typically calibrated against the pressure determined from known ion–molecule reaction kinetics. In the present study, the pressure was determined from the charge-transfer reaction kinetics of toluene-d_8 ions and isotope-selected *p*-bromotoluene ions with *p*-bromotoluene or the reaction kinetics of the benzyl ion with toluene-d_8 and *p*-bromotoluene [36].

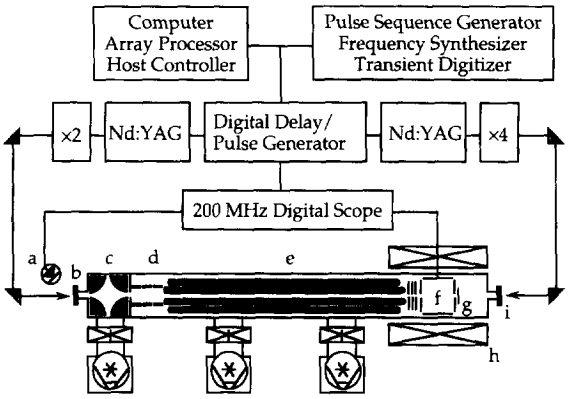

Fig. 1. A Fourier transform ion cyclotron resonance experimental setup for the photoionization charge-transfer and time-resolved photodissociation experiments: (a) photodiode; (b) sapphire window; (c) quadrupole bender; (d) einzel lens; (e) octopole ion guide; (f) 2 inch cubic ICR cell; (g) rhenium filament; (h) superconducting magnet (5 T); (i) calcium fluoride window.

The 266 nm laser beam was from the frequency quadrupled output of an Nd:YAG laser (Spectra-Physics, GCR-150) with a pulse width of ~10 ns. The 532 nm probe laser beam was from the frequency doubled output of an Nd:YAG laser (Continuum, NY-8010) with a pulse width of ~5 ns. The unfocused UV laser beam enters the vacuum chamber through a calcium fluoride window, passes through the center of the ICR cell along the magnetic field axis, and then exits the vacuum chamber though a sapphire window. The probe laser beam

counterpropagates and overlaps with the UV laser beam. The laser beam sizes are adjusted to 2 mm in diameter using irises. The probe laser power was measured using a pyroelectric power meter (Molectron MAX 500A with PM3 head) after passing through the ICR chamber. The probe laser beam reflected from the entrance window was monitored with a fast photodiode (Hammamatsu S1336-44BQ) to provide time-zero. The precise measurement of time-zero is essential for the extraction of dissociation rate constants from the TRPD data. To record a precise timing between the probe laser and radio frequency (rf) excitation pulse, a quad 200 MHz digital oscilloscope (LeCroy 9304M) was used to monitor both the fast photodiode and transmitter outputs. A time jitter problem inherent in the IonSpec control electronics was eliminated by synchronizing a pulse sequence generator with both a frequency synthesizer programmer and a transient digitizer. To reduce other time jitters among various asynchronous devices, a pulse sequence was synchronously controlled by two digital delay/pulse generators (Stanford Research System, DDG-335).

The *p*-bromotoluene ions were generated by either EI (16 ± 1 eV) or PICT. The toluene-d_8 ions produced via 2PI of toluene-d_8 at 266 nm undergo exothermic charge-transfer reactions 3 with *p*-bromotoluene as shown in Fig. 2 {*IP*(toluene) = 8.8276 eV [37] and *IP*(*p*-bromotoluene) = 8.67 eV [9]}.

$$C_6D_5CD_3 + 2h\nu(266\text{ nm}) \rightarrow C_6D_5CD_3^{+\cdot} + e^- \quad (2)$$

$$C_6D_5CD_3^{+\cdot} + p\text{-}CH_3C_6H_4Br \rightarrow p\text{-}CH_3C_6H_4Br^{+\cdot} + C_6D_5CD_3 \quad (3)$$

The rate constant for the charge-transfer reaction is 1.2×10^{-9} cm^3 molecule^{-1} s^{-1}. The subsequent degenerate charge-exchange reactions of the *p*-bromotoluene ions with the parent neutral thermalize the parent ions. Fig. 3 illustrates degenerate charge-exchange reactions

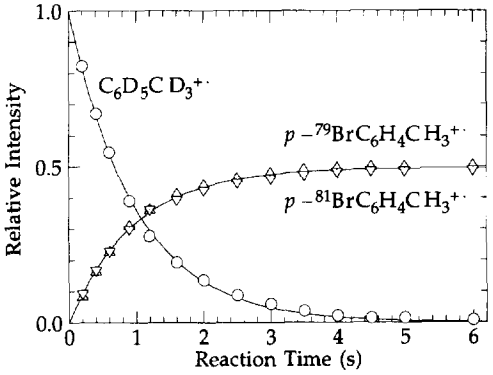

Fig. 2. Charge-transfer reactions of the toluene-d_8 ions with *p*-bromotoluene. The $C_6D_5CD_3^{+\cdot}$ ions were produced by two-photon ionization with a 266 nm laser at time zero. The rate constant for the charge-transfer reaction is 1.2×10^{-9} cm^3 molecule^{-1} s^{-1}. P(toluene-d_8) = 2.9×10^{-8} Torr and P(*p*-bromotoluene) = 2.4×10^{-8} Torr.

of the isotope-selected parent ions with *p*-bromotoluene.

$$p\text{-}CH_3C_6H_4Br^{+\cdot} + p\text{-}CH_3C_6H_4\mathbf{Br} \rightarrow p\text{-}CH_3C_6H_4\mathbf{Br}^{+\cdot} + p\text{-}CH_3C_6H_4Br \quad (4)$$

The rate constant of 1.8×10^{-9} cm^3 molecule^{-1} s^{-1} is close to the collision limit. The direct 2PI of *p*-bromotoluene was not productive because of the fast dissociation of neutral *p*-bromotoluene at 266 nm. The structure of the $C_7H_7^+$ product ion

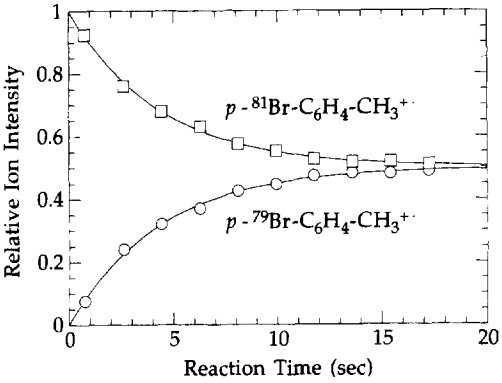

Fig. 3. Degenerate charge-exchange reactions of the $^{81}BrC_6H_4CH_3^{+\cdot}$ ions with the parent neutral [P(bromotoluene) = 1.4×10^{-8} Torr]. The rate constant is 1.8×10^{-9} cm^3 molecule^{-1} s^{-1}. An m/z = 172 disappearance curve represents a least square fit to 1/2[1+exp(− kt/4)], while an m/z = 170 appearance curve represents a least square fit to 1/2[1−exp(−kt/4)].

was identified by ion–molecule reactions. The benzyl ion reacts with toluene-d_8 to yield $CD_3C_6D_4CH_2^+$, while the tropylium ion is unreactive [5].

Both *p*-bromotoluene and toluene-d_8 were obtained from Aldrich and used without further purifications, but after several freeze–pump–thaw cycles.

2.1. The signal equation

The TRPD spectra were obtained by monitoring the appearance of $C_7H_7^+$ as a function of the time delay between the probe laser and the beginning of rf excitation pulse [18]. A typical rf pulse width was 10 or 20 μs and the peak-to-peak amplitude was 50 V. The transient acquisition was 8.192 ms long.

The TRPD ICR signal equations are given in Eqs. (5) and (6) [22].

$$S(t) = C(t+\Delta-t_0)\left\{1-\frac{1-\exp[-k(t+\Delta-t_0)]}{k(t+\Delta-t_0)}\right\} \quad \text{for } t \le t_0 \le t+\Delta, \tag{5}$$

$$= C\Delta\left\{1-\exp[-k(t-t_0)]\frac{1-\exp(-k\Delta)}{k\Delta}\right\} \quad \text{for } t_0 \le t, \tag{6}$$

where $S(t)$ is the product ion signal, C is the proportionality constant, Δ is the rf excitation pulse width, and k is the rate constant. The probe laser is fixed at t_0, while the beginning of rf excitation pulse is scanned. Eqs. (5) and (6) correspond to a timing that the rf excitation begins before and after the probe laser, respectively. The parent ion correction terms are neglected because the dephasing rate in a 5 T magnetic field strength is much faster than the dissociation rate [22].

Since the rate constant k is a function of the internal energy, $k(h\nu + E)$, the signal equation is convoluted with an internal energy distribution of the parent ion at a given initial temperature [20].

$$\langle S(t)\rangle = \sum_{E=0}^{E_0} P(E)S(t) \tag{7}$$

where $\langle S(t)\rangle$ is the convoluted signal equation, E_0 is the lowest dissociation threshold, and $P(E)$ is the probability of having a vibrational energy E at a given initial temperature. Since the parent ion population is depleted above E_0 due to dissociation, $P(E)$ is calculated using a truncated Boltzmann distribution [38,39].

$$P(E) = \frac{\rho(E)\exp(-E/kT)}{Q} \tag{8}$$

$$Q = \sum_{E=0}^{E_0} \rho(E)\exp(-E/kT), \tag{9}$$

where $\rho(E)$ is the density of states of molecule and Q is the vibrational partition function. $\rho(E)$ is obtained by directly counting the number of states in harmonic oscillators. Vibrational frequencies are taken from [9]. The thermal internal energy is significantly modified from the Boltzmann distribution at high temperature as illustrated in Fig. 4 for the *p*-bromotoluene ion [38]. The internal energy of ion is concave downward from 800 K and approaches to E_0 at 1.9 eV.

The TRPD spectra of the parent ion from PICT are analyzed as follows. Firstly, a trial rate–energy curve is used to estimate the temperature

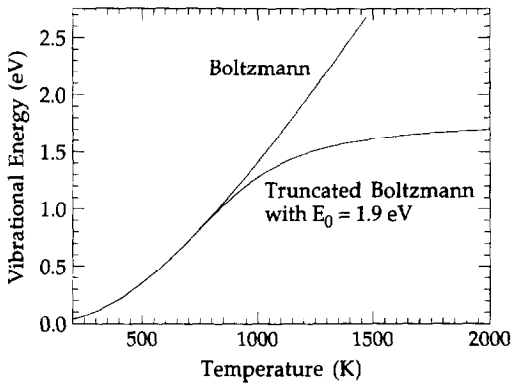

Fig. 4. The vibrational internal energy of the *p*-bromotoluene ion as a function of temperature. The internal energy is concave downward at high temperature due to the truncated vibrational energy level distribution with a threshold at E_0 = 1.9 eV.

of ion by fitting the TRPD data with the convoluted equation. Then, the rate–energy parameters are adjusted iteratively until the temperature of ion becomes the room temperature at 293 K and the rate–energy curve fits both the present result and the PEPICO data [9]. Once the best rate–energy curve is found, it is used for the extraction of the internal temperature of ion from the TRPD data of vibrationally hot ions. The average internal energy is obtained from the truncated Boltzmann temperature–energy curve shown in Fig. 4. The average rate constant represents the RRKM rate at a given average internal energy. Note in passing that a single exponential curve with the average rate constant never fits the TRPD data.

3. Results and discussion

3.1. The structure of the $C_7H_7^+$ product ion

Since the product ions formed within the first 20 μs resulted from two-photon processes, they were ejected out of the ICR cell after 20 μs delay from the laser firing. The rest of $C_7H_7^+$ from the slow one-photon dissociation (1PD) of *p*-bromotoluene ions prepared by PICT reacted with toluene-d_8 to yield $CD_3C_6D_4CH_2^+$, indicating the benzyl ion structure.

$$p\text{-}CH_3C_6H_4Br^{+\cdot} + h\nu(532nm) \rightarrow C_6H_5CH_2^+ + Br \quad (10)$$

$$C_6H_5CH_2^+ + C_6D_5CD_3 \rightarrow CD_3C_6D_4CH_2^+ + C_6H_5D \quad (11)$$

No unreactive components were detected after 20 s reaction time, indicating the absence of the tropylium ion formation from the slow 1PD process. It is concluded that the lowest activation rearrangement process leads to the formation of the benzyl ion exclusively. However, when all $C_7H_7^+$ ions from both one- and two-photon processes were analyzed, there were about 3% of unreactive $C_7H_7^+$ ions detected, meaning that the unreactive tropylium ions resulted from 2PD processes. The relative two-photon yield obtained from the TRPD spectral analysis provides an estimate of ~8% for the relative abundance of the tropylium ion from 2PD.

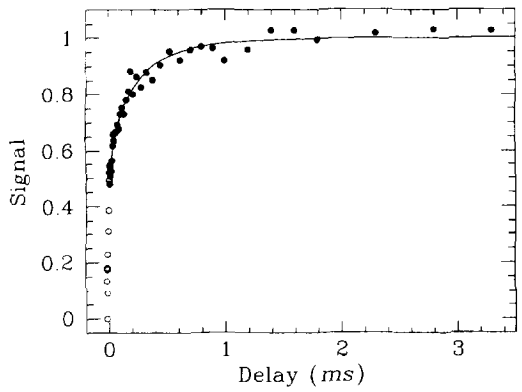

Fig. 5. The TRPD spectra of the *p*-bromotoluene ion at 293 K prepared by PICT with λ = 532 nm and a laser power = ~5 mJ/pulse. The convoluted signal is used to fit the experimental data. The average rate constant for the slow 1PD is $(6 \pm 1) \times 10^3\ s^{-1}$. The rate constant for the 2PD is greater than $5 \times 10^5\ s^{-1}$.

3.2. TRPD of thermal ions and RRKM parameters

Representative TRPD spectra obtained with a laser power of 5 mJ/pulse are shown in Fig. 5 for the *p*-bromotoluene ion derived from PICT at 293 K. The initial fast component rises faster than $(5 \pm 1.6) \times 10^5\ s^{-1}$, which is the detection limit of a 20 μs rf excitation pulse. As the laser power increases, the time-zero intercept at $t = t_0$ increases, which is suggestive of at least two-photon processes. The laser power dependence data are summarized in Table 1. Two-photon

Table 1
The power dependence of the rate of 1PD and the yield of 2PD of the *p*-bromotoluene ion produced by PICT at 293 K.

Laser power (mJ)	k_T (s^{-1})	% Two-photon yield
1.6	8000 ± 1300	24 ± 3
2.4	6000 ± 1000	35 ± 4
5.0	6000 ± 700	46 ± 2
9.5	8000 ± 1300	44 ± 4
> 20	8000 ± 1200	61 ± 5
	$k_{average} = (7 \pm 2) \times 10^3\ s^{-1}$	

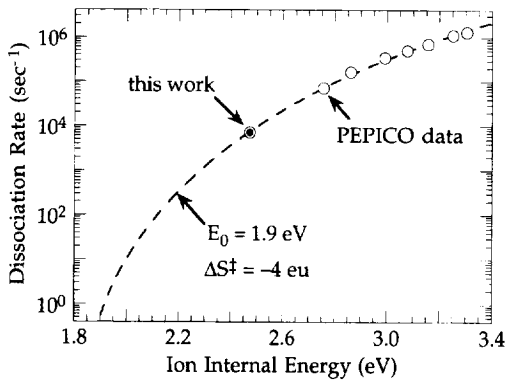

Fig. 6. The RRKM rate–energy curve derived from the average dissociation rate at 532 nm (solid symbol) combined with the PEPICO results (open circle).

yields do not correlate directly to the laser power variation. It appears that a high photon flux produces a hole-burning effect on ion abundances along the laser beam path. The slow components yield almost identical dissociation rates within experimental errors. On average, the rate constant for the slow 1PD is $(7 \pm 2) \times 10^3$ s^{-1} for the ion with an average internal energy of 2.43 eV (the energy of one photon at 532 nm plus thermal energy at 293 K). When combined with PEPICO data [9], our result leads to the RRKM parameters, E_0 = 1.9 eV and $\Delta S^{\ddagger}$(1000 K) = –4 eu. The RRKM rate–energy curve is presented in Fig. 6 along with the experimental data points. In the RRKM fit, the *p*-tolyl ion channel from the

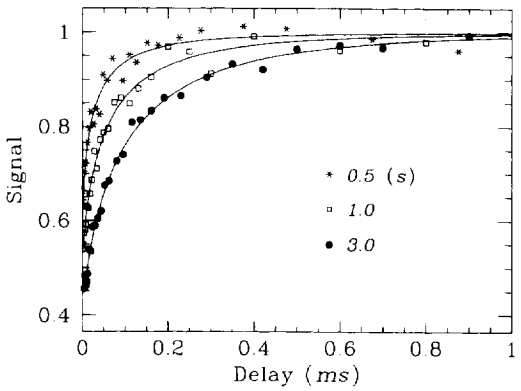

Fig. 7. TRPD spectra of ions from EI as a function of time delay between the electron beam and probe laser pulses. λ = 532 nm and a laser power = ~5 mJ/pulse. The partial pressure of the *p*-bromotoluene is $\sim 1.0 \times 10^{-8}$ Torr.

direct C–Br cleavage with a 2.93 eV threshold is not considered because its contribution to the dissociation rate in the energy range 2.4–3.3 eV is negligible compared with the lowest activation rearrangement channel.

3.3. TRPD of vibrationally hot ions from EI

A series of TRPD spectra of vibrationally hot ions from EI is obtained with increasing cooling time. The overall dissociation rate decreases with increasing cooling time as shown in Fig. 7. The convoluted eqn (7) is used to extract the internal temperature of ions from the best fit to the TRPD data. The average internal energy of ion is obtained from the temperature–energy curve shown in Fig. 4. The results are summarized in Table 2. The two-photon yield remains nearly constant owing to a fixed laser power. The decay of ion internal energy as a function of cooling time is plotted in Fig. 8. Provided that the excess internal energy of ion decays exponentially by eqn (12) [20,22,25,31,40], the cooling time constant for the energy relaxation is determined.

$$E(t) - E(\infty) = [E(0) - E(\infty)] \exp(-t/\tau_{\text{cool}}), \quad (12)$$

where $E(t)$ is the internal energy, $E(0)$ and $E(\infty)$ is the initial internal energy and the relaxed internal energy at thermal equilibrium, respectively. τ_{cool} is the cooling time constant. An estimate for τ_{cool} is 1.0 ± 0.2 s with an initial excess energy of $E(0)$–$E(\infty)$ = 0.34 ± 0.06 eV. The relaxed

Table 2
The cooling of internal energy of ions from EI.[a]

Delay (s)	T (K)	$E(t)$ (eV)[b]	% Two-photon yield
0.50	500 ± 19	0.40 ± 0.033	38 ± 7
0.70	460 ± 16	0.34 ± 0.024	37 ± 6
1.0	420 ± 12	0.28 ± 0.016	37 ± 4
3.0	340 ± 6	0.19 ± 0.007	36 ± 1
20.0	320 ± 8	0.17 ± 0.005	32 ± 2

[a] The partial pressure of *p*-bromotoluene is $\sim 1.0 \times 10^{-8}$ Torr.
[b] The rotational temperature is considered the same as the thermal equilibrium temperature of neutral molecule at 320 K.

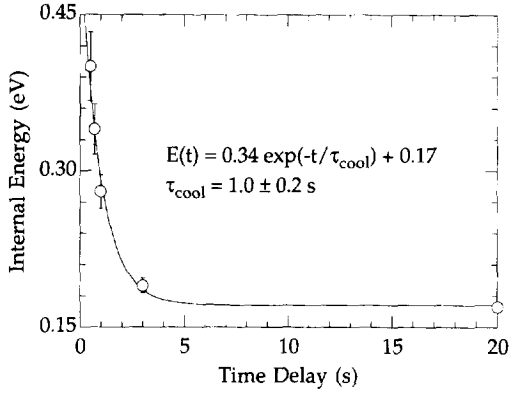

Fig. 8. A plot of ion internal energy as a function of cooling time. The energy cooling time constant is estimated 1.0 ± 0.2 s.

internal energy of $E(\infty)$ = 0.17 ± 0.005 eV corresponds to 320 ± 20 K. The cooling time constant of τ_{cool} = ~1.0 s appears to be quite normal compared to the "average" hydrocarbon ions [2].

Vibrationally hot ions lose their internal energies by the radiative relaxation and collisional quenching processes. To differentiate two contributions, the pressure dependence of TRPD spectra was examined after 0.3 s delay from EI at three different pressures as shown in Fig. 9. The average internal energies extracted from the temperature–energy curve shown in Fig. 4 are listed in Table 3. The rate of exponential cooling of the internal energy is taken as the

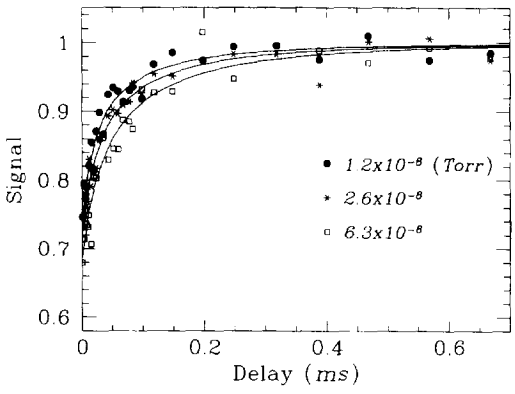

Fig. 9. TRPD spectra of ions from EI as a function of pressure with a fixed time delay of 0.3 s. λ = 532 nm and a laser power = ~5 mJ/pulse.

Table 3
The pressure dependence of ion internal energy.[a]

Pressure (10^{-8} Torr)	T (K)	E_T (eV)	% Two-photon yield
1.2 ± 0.2	480 ± 24	0.37 ± 0.026	59 ± 9
2.6 ± 0.5	450 ± 16	0.32 ± 0.022	60 ± 6
6.3 ± 1.3	420 ± 19	0.29 ± 0.025	58 ± 6

[a] The delay between EI and photolysis was fixed at 0.3 s.

sum of the collisional quenching and radiative relaxation rates as given in Eq. (13) [2].

$$1/\tau_{cool} = k_c[P] + 1/\tau_{rad}, \quad (13)$$

where k_c is the collisional quenching rate constant, $[P]$ is the pressure of collision partner, and τ_{rad} is the radiative relaxation time constant. Substituting Eq. (13) into Eq. (12) with $E(0)$–$E(\infty)$ = 0.34 ± 0.06 eV, $E(\infty)$ = 0.17 ± 0.005 eV, and t = 0.3 s leads to k_c = (0.9 ± 0.5) × 10^{-9} cm^3 molecule^{-1} s^{-1}. Taking values for the initial excess energy and the final relaxed energy predetermined from Fig. 7 helps reduce the uncertainty in the collisional quenching rate constant. The dotted lines in Fig. 10 graphically show the goodness-of-fit in the weighted least-square fitting. The collisional quenching rate constant is fortuitously close to one half the collision-limited rate constant of 1.8 × 10^{-9} cm^3

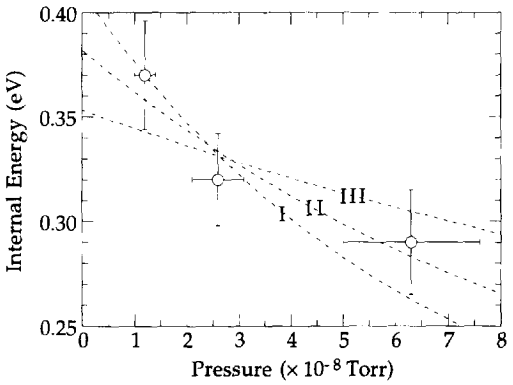

Fig. 10. A plot of ion internal energy as a function of the partial pressure of the *p*-bromotoluene. The dotted lines represent the goodness-of-fit. Curve I: $E(0)$–$E(\infty)$ = 0.40 eV, $E(\infty)$ = 0.17 eV, and k_c = 1.4 × 10^{-9} cm^3 molecule^{-1} s^{-1}; Curve II: $E(0)$–$E(\infty)$ = 0.34 eV, $E(\infty)$ = 0.17 eV, and k_c = 0.9 × 10^{-9} cm^3 molecule^{-1} s^{-1}; Curve III: $E(0)$–$E(\infty)$ = 0.28 eV, $E(\infty)$ = 0.17 eV, and k_c = 0.4 × 10^{-9} cm^3 molecule^{-1} s^{-1}.

molecule^{-1} s^{-1} for the degenerate charge-exchange reaction 4 as expected from the probability of reactive charge-transfer collision. The present result corroborates our earlier notion that the degenerate charge-exchange reaction thermalizes the parent ion. The radiative relaxation time constant can not be determined reliably from the present data. It needs a series of cooling time constant measurements as a function pressure.

3.4. The effect of radiative heating of electron filament

While running TRPD experiments with EI, we noticed that the radiative heating by hot filament affected the dissociation rates. Since the ICR cell compartment is continuously exposed to the thermal radiation from hot filament [39], the ambient temperature of the ICR cell is somewhat higher than the room temperature. The effect of radiative heating on the ion internal energy was investigated as a thermometric probe of the temperature of the ICR cell. The parent ions were prepared by PICT and their TRPD spectra were taken while warming up the ICR cell by hot filament. The results are summarized in Table 4. The overall rate of 1PD increases slowly and reaches the steady value after one and half hours of warming. The temperature of ion at the steady state is estimated to be ~350 ± 20 K, which is considered the temperature of the ICR cell. The ICR cell temperature varies with a filament current.

Table 4
The effect of resistive heating on the ion internal energy.

Exposure (min)	T (K)	E (eV)[a]	% Two-photon yield
0	290 ± 14	0.13 ± 0.013	38 ± 3
30	300 ± 17	0.14 ± 0.015	39 ± 4
60	310 ± 15	0.16 ± 0.015	38 ± 4
90	350 ± 23	0.20 ± 0.024	36 ± 6
120	350 ± 21	0.20 ± 0.023	41 ± 6

[a] The rotational temperature of ion is considered the same as the internal temperature of ion.

3.5. The mechanism of dissociation of the p-bromotoluene ion

One of the most important results is the identification of the structure of $C_7H_7^+$ from the energy-selective dissociation of the *p*-bromotoluene ion. The energy level diagrams are shown in Fig. 11. The 1PD at 532 nm yields the benzyl ion exclusively, while the 2PD produces both the benzyl and tropylium ions. It is suggested that the lowest activation process yields the benzyl ion exclusively, while the direct C–Br cleavage produces the *p*-tolyl ion that isomerizes to both the benzyl and tropylium ions. Comparisons with iodotoluenes provide newer insight into the mechanism of rearrangements. We have recently shown that the lowest activation process of the *p*-iodotoluene ion also yields the benzyl ion exclusively [41]. There are almost no differences in critical activation parameters between the *p*-bromo- and *p*-iodotoluene ions, indicating that halogens are spectators in the rearrangement process [42]. McLafferty and Bockhoff [11] have previously suggested the isomerization of halotoluene ions to halomethylenecyclohexadiene ions to account for the benzyl formation. Our results lend experimental supports to the McLafferty rearrangement mechanism, although the existence of such an

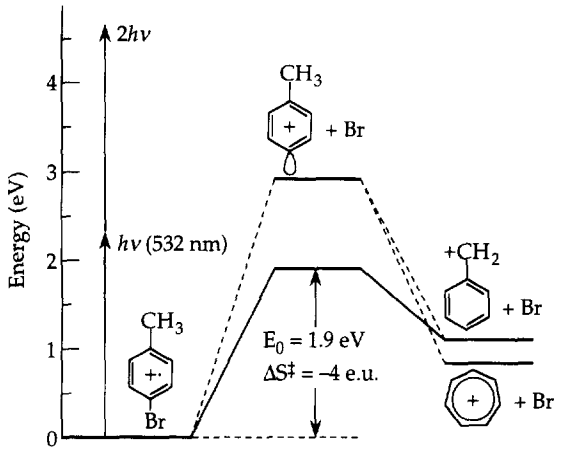

Fig. 11. The energy level diagram of one- and two-photon dissociations of *p*-bromotoluene ion.

intermediate is yet to be observed. They also proposed the isomerization of tolyl ions to the tropylium ion via the benzyl ion formation [11]. However, we found no evidence for the isomerization of the benzyl ion to the tropylium ion. Further investigations are underway to assess the propensity of the tropylium ion formation from *o*-, *m*-, *p*-tolyl ions [41].

4. Conclusion

The photoionization charge-transfer (PICT) process is applied to prepare the thermalized *p*-bromotoluene ions in the ICR cell in the absence of radiative heating by hot filament. The PICT method is especially useful in the case where the direct multiphoton ionization is not productive due to the dissociation of the parent neutral in the excited state. The energy-selective preparation of the parent ion by PICT and the subsequent photoexcitation allow the energy-selective characterization of the unimolecular dissociation of the parent ion. One-photon excitation of the *p*-bromotoluene ion at 532 nm induces the intramolecular rearrangement to the exclusive formation of the benzyl ion with a loss of Br, while two-photon excitation involves a direct C–Br cleavage that leads to the *p*-tolyl ion which isomerizes to both the benzyl and tropylium ions.

The time-resolved photodissociation spectroscopy is used to probe the internal energy of ions from EI. Vibrationally hot ions relax to thermal equilibrium populations by the collisional quenching and radiative relaxation processes. The degenerate charge-exchange reaction is very efficient in collisional thermalization. The radiative heating of an ICR cell by hot filament raises the temperature of neutral molecules in the ICR cell significantly, thereby increasing the internal energy of thermalized ions. Most of the electron impact studies of ion–molecule reactions are considered as hot ion chemistry.

Acknowledgements

This work was supported by the National Science Foundation Grant No. CHE-9302959, the National Science Foundation Young Investigator Award CHE-9457668, the Arnold and Mabel Beckman Foundation Young Investigator Award, and the Petroleum Research Fund Grant No. 25423-G3. This work was also made possible by the Santa Barbara Laser Pool under NSF Grant No. CHE-9413030.

References

[1] T. Baer, Adv. Chem. Phys., 64 (1986) 111.
[2] R.C. Dunbar, Mass Spectrom. Rev., 11 (1992) 309, and earlier references therein.
[3] T. Baer, In: M.T. Bowers (Ed.), Gas Phase Ion Chemistry, Vol. 1, Academic Press, New York, 1979.
[4] S.L. Anderson, Adv. Chem. Phys., 82 (1992) 177.
[5] J.-A.A. Jackson, S.G. Lias and P. Ausloos, J. Am. Chem. Soc., 99 (1977) 7515.
[6] F.W. McLafferty and J. Winkler, J. Am. Chem. Soc., 96 (1974) 5182.
[7] C.J. Proctor and F.W. McLafferty, Org. Mass Spectrom., 18 (1983) 193.
[8] B.J. Stapleton, R.D. Bowen and D.H. Williams, J. Chem. Soc., Perkin Trans. 2, (1979) 1219.
[9] S. Olesik, T. Baer, J.C. Morrow, J.J. Ridal, J. Buschek and J.L. Holmes, Org. Mass Spectrom., 24 (1989) 1008.
[10] R.C. Dunbar, J.P. Honovich and B. Asamoto, J. Phys. Chem., 92 (1988) 6935.
[11] F.W. McLafferty and F.M. Bockhoff, Org. Mass Spectrom., 14 (1979) 181.
[12] J.C. Choe and M.S. Kim, Int. J. Mass Spectrom. Ion Processes, 107 (1991) 103.
[13] R.C. Dunbar and C. Lifshitz, J. Chem. Phys., 94 (1991) 3542.
[14] C. Lifshitz, I. Levin, S. Kababia and R.C. Dunbar, J. Phys. Chem., 95 (1991) 1667.
[15] C.Y. Lin and R.C. Dunbar, J. Phys. Chem., 98 (1994) 1369.
[16] Y.S. Cho, M.S. Kim and J.C. Choe, Int. J. Mass Spectrom. Ion Processes, 145 (1995) 187.
[17] J. Shen, R.C. Dunbar and G.A. Olah, J. Am. Chem. Soc., 96 (1974) 6227.
[18] R.C. Dunbar, J. Phys. Chem., 91 (1987) 2801.
[19] H.Y. So and R.C. Dunbar, J. Am. Chem. Soc., 110 (1988) 3080.
[20] J.D. Faulk, R.C. Dunbar and C. Lifshitz, J. Am. Chem. Soc., 112 (1990) 7893.
[21] F.S. Huang and R.C. Dunbar, Int. J. Mass Spectrom. Ion Processes, 109 (1991) 151.
[22] R.C. Dunbar, J. Chem. Phys., 91 (1989) 6080.
[23] R.C. Dunbar, J. Am. Chem. Soc., 111 (1989) 5572.

[24] J.D. Faulk and R.C. Dunbar, J. Phys. Chem., 95 (1991) 6932.
[25] Y.P. Ho and R.C. Dunbar, J. Phys. Chem., 97 (1993) 11474.
[26] Y.P. Ho, R.C. Dunbar and C. Lifshitz, J. Am. Chem. Soc., 117 (1995) 6504.
[27] J.D. Faulk and R.C. Dunbar, J. Am. Chem. Soc., 114 (1992) 8596.
[28] F.S. Huang and R.C. Dunbar, J. Am. Chem. Soc., 112 (1990) 8167.
[29] G.H. Weddle, R.C. Dunbar, K.S. Song and T.H. Morton, J. Am. Chem. Soc., 117 (1995) 2573.
[30] Y. Gotkis, M, Naor, J. Laskin, C. Lifshitz, J.D. Faulk and R.C. Dunbar, J. Am. Chem. Soc., 115 (1993) 7402.
[31] C.Y. Lin and R.C. Dunbar, J. Phys. Chem., 99 (1995) 1754.
[32] R.T. McIver Jr., Rev. Sci. Instrum., 41 (1970) 555.
[33] M.B. Comisarow, Int. J. Mass Spectrom. Ion Phys., 37 (1981) 251.
[34] G. Shenheng and A.G. Marshall, Int. J. Mass Spectrom. Ion Processes, 146 (1995) 261.
[35] G.J. Schulz and A.V. Phelps, Rev. Sci. Instrum., 28 (1957) 1051.
[36] P. Ausloos, J.-A.A. Jackson and S.G. Lias, Int. J. Mass Spectrom. Ion Phys., 33 (1980) 269.
[37] K.T. Lu, G.C. Eiden and J.C. Weisshaar, J. Phys. Chem., 96 (1992) 9742.
[38] R.C. Dunbar, J. Chem. Phys., 95 (1991) 2537.
[39] R.C. Dunbar, J. Phys. Chem., 98 (1994) 8705.
[40] R.C. Dunbar, J. Chem. Phys., 90 (1989) 7369.
[41] S.K. Shin, B. Kim, S.-J. Han and R.L. Jarek, Chem. Phys. Lett., in press.
[42] B. Kim and S.K. Shin, J. Chem. Phys., in press.